




## Complex quantum network models from spin clusters

Ravi T. C. Chepuri <sup>1,2</sup> & István A. Kovács <sup>1,3</sup> 

In the emerging quantum internet, complex network topology could lead to efficient quantum communication and robustness against failures. However, there are concerns about complexity in quantum communication networks, such as potentially limited end-to-end transmission capacity. These challenges call for model systems in which the impact of complex topology on quantum communication protocols can be explored. Here, we present a theoretical model for complex quantum communication networks on a lattice of spins, wherein entangled spin clusters in interacting quantum spin systems serve as communication links between appropriately selected regions of spins. Specifically, we show that ground state Greenberger-Horne-Zeilinger clusters of the two-dimensional random transverse-field Ising model can be used as communication links between regions of spins. Further, the resulting quantum networks can have complexity comparable to that of the classical internet. Our work provides a generative model for further studies towards determining the network characteristics of the emerging quantum internet.

<sup>1</sup>Department of Physics and Astronomy, Northwestern University, Evanston, IL 60208, USA. <sup>2</sup>Department of Physics, University of Maryland, College Park, MD 20742, USA. <sup>3</sup>Northwestern Institute on Complex Systems, Northwestern University, Evanston, IL 60208, USA. ✉email: [istvan.kovacs@northwestern.edu](mailto:istvan.kovacs@northwestern.edu)

The creation of a global quantum communication network to serve as a quantum internet is a highly anticipated goal that would enhance the existing classical internet, with applications in secure communications, quantum computation, distributed sensing, and more<sup>1–4</sup>. Experimental advances toward the technology needed for a quantum internet, such as quantum repeaters, are rapidly being made<sup>5–12</sup>. Such advances have already enabled the creation of quantum communication networks with a few nodes, which may be precursors to the future quantum internet<sup>2,13–15</sup>.

In the simplest case of quantum repeater based architectures, quantum communication networks can be represented as shown in Fig. 1a<sup>16–22</sup>. Each node of the network represents a collection of quantum bits, or qubits, and each link of the network represents an entangled pair of qubits belonging to two distinct nodes. As such, the degree of each node (the number of links it has) is at most the number of qubits in the node. Although non-adjacent nodes such as *A* and *C* in Fig. 1a do not share entangled qubits, strategic local quantum operations on the qubits of the intermediate node *B* can create entanglement between qubits of *A* and *C* in a process known as entanglement swapping. Quantum routing protocols based on entanglement swapping can generate entanglement between even more distant nodes, thereby enabling quantum communication between remote pairs of nodes within the network<sup>17,20–24</sup>.

Complex network topology is an emergent property observed in diverse real world networks. Complex networks prominently exhibit a heavy-tailed degree distribution, approximated by a power-law as

$$P(k) \propto k^{-\gamma} \quad (1)$$

with  $2 < \gamma < 3$ , where  $k$  is the degree of the node and  $P(k)$  is the fraction of nodes having degree  $k$ <sup>25</sup>. Another key feature of network complexity is the small-world property, stating that other nodes can be reached in a few steps from any given node: the

diameter  $d$  of the network (the maximum shortest path length between any two nodes) increases slower than a power-law, for example  $d \propto \ln N$  for a network of  $N$  nodes. Complex topology has been shown to be essential to the proper functioning of the classical internet, for instance by making it robust to the random failure of computers or routers<sup>26</sup>.

Recent findings highlight the need to investigate the possibility of complex topology in a quantum internet. For example, complex quantum communication networks exhibit promising robustness to random failures of noisy quantum-repeater nodes<sup>27</sup> (though in the different framework of quantum spin models on imprinted networks, complexity does not necessarily provide robustness<sup>28</sup>). Additionally, satellite-based quantum networks naturally have the small world property, meaning only a few entanglement swaps are needed to enable communication between any pair of nodes<sup>29</sup>. This is advantageous due to reduced usage of quantum resources. Another advantage to complex topology is that existing optical cables of the classical internet could be utilized for quantum communication, likely as part of a hybrid architecture along with more expensive cryo-cables, thus providing incentive to eventually match (at least partially) the complex topology of the classical internet<sup>4–6,30</sup>.

However, there are also anticipated difficulties with creating quantum communication networks that mimic the complexity of the classical internet. For one, unlike in the case of satellite-based quantum networks, quantum networks based on optical fibers do not necessarily have the small world property due to photonic losses limiting transmission length<sup>31</sup>. There are also concerns that low network densities of complex networks may limit end-to-end transmission capacity of quantum information, and that there is vulnerability to targeted attacks, just as in the classical internet<sup>32,33</sup>. By default, existing proposals for the creation of quantum communication networks avoid these issues by imposing a simple, grid-like network structure<sup>1,3</sup>. Further, existing quantum routing protocols often assume simple grid-like or

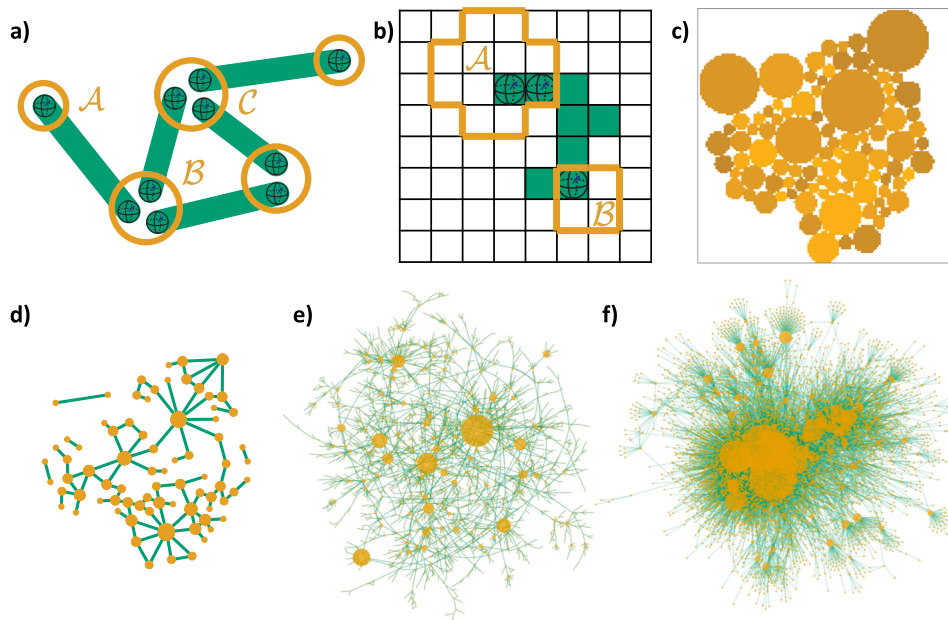


**Fig. 1** Creation of quantum networks using spin clusters. **a** Quantum communication networks based on quantum repeaters consist of collections of local qubits (orange nodes) that are entangled (green links) with qubits in other local collections. **b** We propose the use of entangled clusters (green) in interacting spin systems as communication channels between nodes that are spatially localized regions of lattice sites (orange). **c** Nodes are chosen as adjacent circular regions of sites from a broad size distribution, as illustrated here on a lattice of size  $128 \times 128$ . A link is added when a cluster in the underlying spin system is shared by exactly two nodes. **d** The resulting network between nodes in panel (c) indicates which pairs of nodes share entanglement. **e** Using larger lattices (here  $4096 \times 4096$ ), a complex network emerges. **f** A snapshot of the classical internet from 1999 at the level of autonomous systems<sup>62</sup> shows similar complexity to that in panel (e), although being significantly larger.

ring-like network structure<sup>17,20,21,23</sup>, with one recent exception<sup>24</sup>. As such, there is a need for model systems in which the impact of complex topology on quantum communication can be studied.

In this paper, we present a proof-of-concept model to create quantum networks of substantial complexity in the context of spins on a lattice. In spin models on a two-dimensional lattice such as the two-dimensional random transverse-field Ising model (RTIM), there is a dominance of disorder near the critical point<sup>34–40</sup>. The emerging strong disorder physics induces locality, causing the ground state of the system to factorize into distinct entangled Greenberger-Horne-Zeilinger (GHZ) spin clusters (each corresponding to a magnetic domain)<sup>39–43</sup>. Here, we propose interpreting the emergent GHZ clusters as links of a quantum network: we choose regions of the lattice as nodes, and link two nodes if a spin cluster overlaps both node regions and no other node regions, as shown in Fig. 1b. We find that the resulting quantum networks can have substantial complexity similar to that observed for the classical internet. Our work is in part inspired by a previous study<sup>44</sup>, in which the author studied superconductivity by viewing clusters as nodes and adding a link between clusters if they were sufficiently close together. We focus primarily on the prominent example of the critical 2D RTIM, but our results apply generally to systems exhibiting strong disorder.

## Results

**Quantum network construction.** In this work, ground-state spin clusters of the RTIM serve as links for constructing complex quantum networks. As an overview of our construction, network nodes are chosen to be connected regions of lattice sites, with a broad distribution of sizes, for example as shown in Fig. 1c. Then, nodes are connected by a quantum link if they both have a site belonging to the same spin cluster, and that cluster has no sites in another node, as shown in Fig. 1b.

The two-dimensional RTIM is specified by the Hamiltonian

$$\mathcal{H} = -\sum_{\langle ij \rangle} J_{ij} \sigma_i^x \sigma_j^x - \sum_i h_i \sigma_i^z, \quad (2)$$

where each  $\sigma_i^\alpha$  is the spin-1/2 Pauli matrix in the  $\alpha$  direction for a spin at site  $i$  of a  $L \times L$  square lattice with periodic boundary conditions. The label  $\langle ij \rangle$  indicates that the sum is taken over neighboring sites  $i$  and  $j$  on the lattice, which are coupled by bonds of random strength  $J_{ij} \geq 0$ , each drawn independently from the uniform distribution on the unit interval. Each site  $i$  has a transverse external magnetic field of strength  $h_i$ . The relevant physics of the RTIM remains unchanged for any non-singular distribution of  $h_i$  and  $J_{ij}$  as long as at least the  $h_i$  fields or the  $J_{ij}$  bonds are chosen randomly<sup>45,46</sup>. Therefore, to simplify the model we consider a fixed- $h$  model with a uniform magnetic field  $h_i = h$  for all sites<sup>34,35</sup>, unless otherwise stated.

The RTIM is a paradigmatic example of a system which can undergo a quantum phase transition at zero temperature as the quantum control parameter  $\theta = \ln h$  is tuned past its critical value  $\theta_c$ <sup>47,48</sup>. Below  $\theta_c$  the ground state has a macroscopic spin cluster ordered by the couplings  $J_{ij}$ , and above  $\theta_c$  the ground state is given by small spin clusters aligned independently. In contrast, at the critical point  $\theta_c = -0.17034(2)$ , the spin clusters have a broad size-distribution and are self-similar fractal-like objects<sup>34,35</sup>. Many properties of the critical RTIM are universal<sup>45,46</sup>, that is, they are independent of the form of the disorder in  $h$  and  $J$ , as well as of the type of the 2D lattice.

The ground state of the RTIM can be conveniently determined using the strong disorder renormalization group (SDRG) method<sup>45,46,49,50</sup>, which is asymptotically exact in the vicinity of the critical point<sup>51</sup> as demonstrated in both two and higher dimensions<sup>34–41,52,53</sup>. We used an efficient SDRG algorithm, which runs in  $O(N \log N)$  time for  $N = L^2$  sites, to generate

instances of RTIM ground state clusters at the critical point<sup>34,53</sup>. During the SDRG method, the largest local terms in the Hamiltonian are successively eliminated and new Hamiltonians are generated through a perturbation calculation<sup>34</sup>. After decimating all degrees of freedom, the ground state of the RTIM is found to be a collection of independent ferromagnetic clusters of various size, each cluster being in a GHZ state

$$\frac{1}{\sqrt{2}} (\underbrace{|\uparrow \cdots \uparrow\rangle}_{n \text{ times}} + \underbrace{|\downarrow \cdots \downarrow\rangle}_{n \text{ times}}) \quad (3)$$

where  $\uparrow$  ( $\downarrow$ ) for site  $i$  labels the  $+1$  ( $-1$ ) eigenstate of  $\sigma_i^x$ , and  $n$  is the number of spins in the cluster<sup>42,45,46</sup>. In practice, we considered lattices up to size  $L = 4096$ , with at least 16 instances at each size. An advantage of using the critical point is that it is expected to yield relatively large network size, while the SDRG remains asymptotically exact. Note that the ground state of the RTIM factorizes into a collection of independent GHZ clusters even outside the critical point<sup>42</sup>, indicating that off-critical RTIMs could also be used.

We propose the selection of spatially localized regions of the RTIM lattice to serve as nodes of a model quantum network. This can be motivated by interpreting the RTIM as a model of a magnetic solid: due to temporal restrictions, the magnetic solid may only permit simultaneous quantum operations across small distances. With the lattice partitioned into many local regions, each region may permit local operations on its own sites, much like a node of a real quantum network. In contrast, sites in distant pairs of regions are not in general able to be simultaneously measured.

Consider one spatially localized region  $\mathcal{A}$  of the RTIM lattice that will serve as a network node. The entanglement entropy

$$S = -\text{Tr}(\rho_{\mathcal{A}} \log_2 \rho_{\mathcal{A}}), \quad (4)$$

which is the von Neumann entropy of the reduced density matrix  $\rho_{\mathcal{A}}$ , provides a quantification of the entanglement between  $\mathcal{A}$  and the rest of the lattice  $\mathcal{A}^c$ . Thus,  $S$  is a measure of the node's ability to share entanglement with other nodes. In the RTIM, the entanglement entropy is simply the number of clusters with spins in both  $\mathcal{A}$  and  $\mathcal{A}^c$ <sup>39,41,43,54</sup>, which as a special case of the area law is on average proportional to the surface area (boundary length) of  $\mathcal{A}$ <sup>55</sup>. As a consequence, regions with a larger boundary have a larger capacity to establish connections, leading to a proportionally larger expected degree.

To achieve a heavy-tailed degree distribution for the eventual quantum networks, we aimed to choose node regions with a broad distribution of surface area. As a simple choice, we selected discretized circles of varying sizes in the RTIM lattice as our regions, as shown in Fig. 1c. We chose to sample the circles' radii from a power-law distribution with exponent  $\gamma_{\text{radius}} = 2.67$ . (Other values of  $\gamma_{\text{radius}}$  between 2 and 3 give qualitatively similar results.) A minimum radius of 2 lattice units was used to ensure the circles would consist of at least a few lattice sites. We then placed the circles on the lattice by sequentially placing circles in an outward-spiralling manner so that a new circle is tangent to one or more of the already placed circles<sup>56</sup>. The close placement of the circles in principle promotes connectivity. Note that this method does not attempt to solve the challenging problem of maximizing the packing density, nor is it a uniformly random placement of the circles. In practice, circles were added until a fixed proportion, here chosen to be 0.3, of the lattice sites were covered, as illustrated in Fig. 1c.

Now, with spatially localized regions of the lattice identified as nodes of a model quantum network, we aim to add a link between a pair of nodes  $\mathcal{A}$  and  $\mathcal{B}$  (Fig. 1b) if lattice sites of  $\mathcal{A}$  and  $\mathcal{B}$  share entanglement. Unfortunately, as we partition the system into

more than two subsystems ( $\mathcal{A}$ ,  $\mathcal{B}$ , and the rest of the lattice), it becomes challenging to quantify quantum entanglement between pairs of subsystems<sup>57</sup>, as the entanglement entropy is no longer applicable. As an alternative, one can consider the logarithmic negativity, which is an upper bound for the distillable entanglement. Although the logarithmic negativity is notoriously difficult to compute in practice<sup>58,59</sup>, in the RTIM, the entanglement negativity is non-zero if and only if  $\mathcal{A}$  and  $\mathcal{B}$  share a spin cluster that has no sites outside of these two regions<sup>60,61</sup>. As such, a cogent proposal would be to add a link between  $\mathcal{A}$  and  $\mathcal{B}$  in the quantum network if and only if there exists a cluster that (i) has a spin in both  $\mathcal{A}$  and  $\mathcal{B}$  and (ii) does not have a spin outside of  $\mathcal{A}$  or  $\mathcal{B}$ .

However, the strict construction described above is overly restrictive in the context of quantum networks, as any cluster that has sites in both regions can be used for communication, as long as the other sites in the cluster remain unchanged. As it is reasonable to assume that spins are only manipulated inside the nodes, we chose to add a quantum link between  $\mathcal{A}$  and  $\mathcal{B}$  if and only if there exists a cluster that (i) has a spin in both  $\mathcal{A}$  and  $\mathcal{B}$  and (ii) does not have a spin in a node other than  $\mathcal{A}$  or  $\mathcal{B}$ . Note that in our construction  $\mathcal{A}$  and  $\mathcal{B}$  are typically spatially adjacent and at least some of the shared clusters are relatively small, meaning that in practice this modification has a negligible effect.

If the resulting network is disconnected (as in Fig. 1d), we considered only the largest connected component (LCC) of the network. In other words, each connected component is a separate quantum communication network, and we only consider the largest here.

**Topological analysis of quantum networks.** Visualizations of quantum networks constructed using the method of the previous subsection (Fig. 1e) indicate nontrivial topological features, including highly connected hubs and clustering. This suggests the presence of network complexity, which we verify here numerically. For comparison, we also consider grid-like benchmark networks lacking complexity: quantum networks constructed using the method of the previous subsection but with uniformly sized nodes. In this grid-like benchmark, the radius of the nodes was set so that we have the same overall coverage of the RTIM lattice as in our complex quantum networks. The nodes were arranged in a hexagonal packing on the lattice, and as such the resulting networks are expected to approximate a triangular grid. We also compare to the topology of the classical internet at the level of autonomous systems from 1997 until 2000<sup>62</sup>. From 733 available snapshots we selected five representative networks to serve as a basis for comparison, the earliest of which is visualized in Fig. 1f.

We first check that the quantum networks have a heavy-tailed degree distribution, a hallmark property of network complexity. As the node size distribution obeys a power-law, the expectation based on the area law is that the degree distribution obeys a power-law with the same exponent, under the assumption that node positions were chosen truly randomly. Indeed, Fig. 2a shows a degree distribution of a typical quantum network constructed using the methods of the previous subsection, with a power-law exponent approximately the same as the one by which the node sizes were chosen. A slight difference in the power-law exponent may be attributed to the non-uniformly random selection of the node regions. The degree distribution is qualitatively similar to that of a representative network of the classical internet at the autonomous systems level, while contrasting with grid-like benchmark networks. The inset in Fig. 2a displays an even more clear power-law behavior, upon averaging the degree distribution for a set of quantum networks.

Another key feature of complex networks is the small-world property. Here, we used the average shortest path length  $\langle d \rangle$  between two nodes as a proxy for the diameter of the quantum networks, shown in Fig. 2b for quantum networks from different RTIM system sizes. Though the average path length of the quantum networks is larger than that of the classical internet networks, and also grows slightly faster than  $\langle d \rangle \propto \ln N$ , it is evident that it scales much more slowly than in the grid-like network, which has  $\langle d \rangle \propto \sqrt{N}$ . We conclude that the quantum networks are nearly small-world, although with a somewhat larger diameter than the classical internet.

A closer examination of individual quantum networks reveals that spatially large nodes do not always have a high degree. Depending on the number and size of the surrounding nodes, a large node can often end up with only a few connections, especially if the node is on the periphery of the node packing configuration, or if it is next to other large nodes. We therefore checked for the presence of degree correlations between linked nodes. In Fig. 2c the average degree of a node's nearest neighbors is shown as a function of the node's own degree. Just like in the classical internet, the negative slope indicates that the quantum networks are disassortative, meaning high degree nodes tend to connect to low degree nodes and vice versa. This contrasts with the grid-like benchmark networks, which exhibit approximately neutral behavior. The observed network disassortativity can be quantified by the degree correlation coefficient  $r$ , defined as the Pearson correlation coefficient between degrees at the ends of a link. A correlation coefficient  $r = 0$  means no degree correlations, while negative values indicate disassortativity. A plot of  $r$  against network size in Fig. 2d shows that both the quantum networks and the classical internet exhibit disassortativity for all  $N$ , but they tend to become less disassortative as  $N$  increases. In contrast, grid-like networks have asymptotically no degree correlations. For small sizes, low degree nodes often appear next to each other in areas dominated by a large cluster in the RTIM, as well as on the periphery of the grid, leading to slightly positive  $r$  values.

Degree correlations capture patterns at the level of pairs of connected nodes, but it is often useful to go one step beyond and check patterns of three nodes. The simplest such measurement is the global clustering coefficient, given by

$$C \equiv \frac{3 \cdot \text{Number of complete triangles}}{\text{Number of connected triplets of nodes}} = \frac{\sum_{i,j,k} A_{ij} A_{jk} A_{ki}}{\sum_i k_i (k_i - 1)} \quad (5)$$

where  $A$  is the adjacency matrix of the network. The global clustering coefficient of quantum networks of various sizes are shown in Fig. 2e. A perfect triangular lattice would achieve  $C = 0.4$ , somewhat above the grid-like benchmark networks that often miss some connections. The clustering coefficient of classical internet networks falls into the range spanned by the heterogeneous and grid-like benchmark networks.

Beyond the global clustering coefficient, we can determine if the network exhibits hierarchical modularity, in which low degree nodes tend to exist in dense communities while high degree nodes connect disparate communities, by examining the relationship between the local clustering coefficient and node degree. The local clustering coefficient of node  $i$  is

$$C_{\text{local},i} = \frac{\sum_{j,k} A_{ij} A_{jk} A_{ki}}{k_i (k_i - 1)}. \quad (6)$$

Hierarchical network structure is indicated by a local clustering coefficient that decays as the node degree increases. As shown in Fig. 2f, we indeed observe that  $C_{\text{local}}$  decays with  $k$  in both the quantum networks and the classical internet network. Further, the local clustering coefficient of the quantum networks obeys the

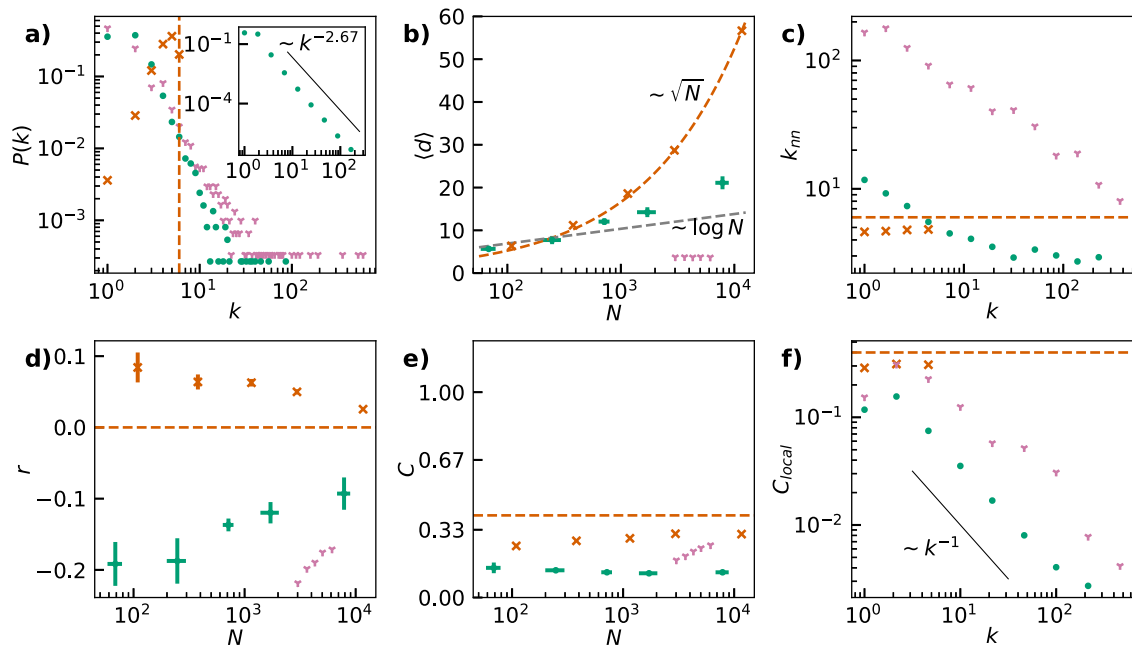


**Fig. 2 Analysis of quantum network topology.** **a** Degree distribution of a quantum network created with heterogeneously sized (green circles,  $N = 3731$  nodes) or uniformly sized (dark orange crosses,  $N = 11,658$ ) circular nodes on a  $4096 \times 4096$  random transverse-field Ising model (RTIM) lattice, and the degree distribution of the classical internet at the autonomous systems level on 11/08/1997 (purple 'Y's,  $N = 3015$ )<sup>62</sup>. The dashed line is the expectation for a triangular grid. Inset: The average degree distribution of 16 quantum networks appears to obey a power-law with exponent approximately the same as that of the node size distribution. **b** Average shortest path length of networks from a few RTIM lattice sizes. Error bars represent standard error of the mean. **c** Average nearest neighbor degree as a function of node degree (averaged over nodes binned logarithmically by degree). **d** Degree correlation coefficients at a few sizes. **e** Global clustering coefficient. **f** Local clustering coefficient vs. degree (averaged over nodes binned logarithmically by degree).

relation  $C_{local} \sim k^{-1}$  well, indicating agreement with the hierarchical network model<sup>63</sup>. Thus the quantum networks share the hierarchical nature of the classical internet, in stark contrast to grid-like networks with no hubs.

**Off-critical RTIM and other variants.** Our approach can be generalized to systems other than the critical fixed- $h$  RTIM discussed above. Starting with an off-critical version, in Fig. 3a, d we perform the construction of the “Quantum network construction” subsection with the control parameter  $\theta$  at various values away from  $\theta_c$ , and plot the average size (number of links) of the LCC of the resulting network. For  $\theta$  near but not at  $\theta_c$ , the network construction still produces quantum networks of substantial size with similar properties and complexity to that found in the previous subsection. We also perform a similar construction with the box- $h$  RTIM, where the  $h_i$  are uniformly distributed in  $(0, h]$ , in Fig. 3b, e. Note that the box- $h$  system has a low density of clusters and typically small clusters, leading to much smaller networks on average. Nonetheless, we still expect to see complexity at larger scales. For both fixed- $h$  and box- $h$  constructions, the network size achieves a maximum for  $\theta \approx \theta_c$ , although this is a coincidence as criticality is not required in our network construction. What we need is a maximum number of local clusters, which happens to occur in the vicinity of the critical point.

To illustrate that criticality is not necessarily required or optimal for our network construction, we consider further variants of the RTIM, such as the diluted RTIM ( $J_{ij} = J \gg h$  with probability  $p$ ,  $J_{ij} = 0$  otherwise)<sup>64–67</sup>. This system has connected ground state clusters in the shape of bond percolation clusters, shown in Fig. 3c, f, and belongs to a different universality class than the fixed- $h$  and box- $h$  RTIM<sup>42,43</sup>. Yet, our network construction still leads to large networks of substantial complexity. Clearly, the maximum network size is achieved far from criticality.

More generally, the quantum network construction can be extended to any system with a ground state that factorizes into independent spin clusters. Such systems include the random Potts and clock models<sup>68</sup> as well as the Ashkin-Teller model<sup>69</sup>.

## Discussion

In this work, we have introduced a theoretical method to create model quantum communication networks on a lattice of spins using entangled clusters as quantum communication channels. Specifically, we have shown that ground state GHZ clusters of the critical RTIM can be used as quantum communication links between local regions of spins, yielding quantum networks with substantial network complexity.

As an extension, spin clusters of different layers could serve both as nodes and links. For example, one layer of the diluted critical RTIM (with percolation clusters) could define the nodes, while another layer could provide the links. As clusters in the critical diluted RTIM have a broad power-law size distribution with exponent  $187/91$ , they would naturally lead to a broad degree distribution<sup>70</sup>.

Our network construction can lead to even more dense and potentially more complex networks by using multiple layers of spin clusters for links. This idea leads to multilayer networks<sup>71</sup>, where the union of the links coming from different layers can increase the topological complexity further, no longer resulting in the current, quasi-planar graphs. In both a single-layer and multilayer construction, we can construct a weighted network, where the link weight is the multiplicity of the established quantum channels between each node pair. While for a purely topological analysis such weights are irrelevant, they can be of key importance for practical quantum communication protocols<sup>27</sup>.

In our model, we focus on pairwise interactions between nodes of the network by discarding clusters with sites in more than two node regions. However, one could in principle keep these clusters

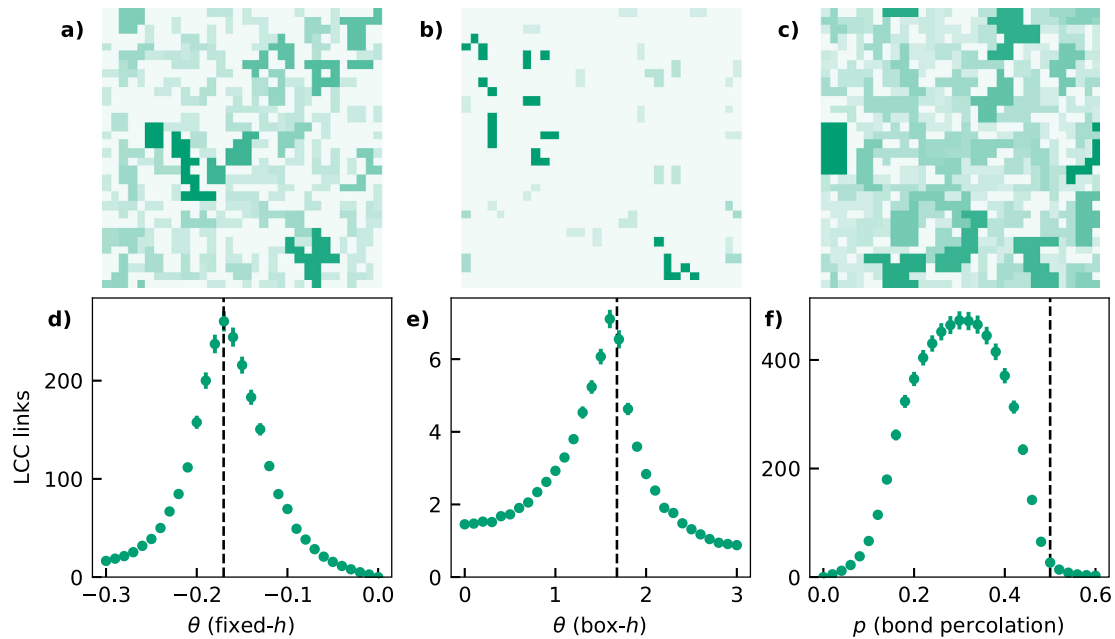


**Fig. 3 Spin clusters in variants of the random transverse-field Ising model (RTIM) used to create quantum networks.** **a** Fixed- $h$  RTIM ground state clusters at the critical  $\theta$ . Clusters are colored by size, and may be disconnected<sup>42,43</sup>. **b** Box- $h$  RTIM ( $h_i$  uniformly distributed in  $(0, h]$ ) ground state clusters at critical  $\theta$ . **c** Bond percolation clusters, which are ground state clusters of the diluted RTIM ( $J_{ij} = J \gg h$  with probability  $p$ ,  $J_{ij} = 0$  otherwise)<sup>64–67</sup>. Here  $p = 0.3$ . **d–f** For each system (here on a  $512 \times 512$  square lattice), there is an optimal value of a cluster control parameter which produces the maximum largest connected cluster (LCC) (averaged over 256 samples; error bars represent standard error of the mean). In the first two cases the optimal value of  $\theta$  approximately coincides with the critical point (dashed lines), but this does not hold in general.

as higher order interactions of a hypergraph, with these interactions representing multipartite quantum entanglement. The resulting quantum hypergraph could be an interesting object for future study, as the creation and distribution of multipartite entangled states on quantum networks is of interest for quantum information processing<sup>22</sup>.

Note that scale-free spatial networks would traditionally require long-range connections<sup>27</sup>. As our design includes spatially extended nodes, scale-free quantum networks can be achieved even with only short range connections, like in the optimal off-critical construction in Fig. 3f. Our quantum network construction could also generalize to higher dimensions. In 3D, the area law means that the degree distribution is coupled to the distribution of the area of the subsystems instead of their linear extent. Hence the degree distribution is expected to obey a power-law with an exponent one larger than the exponent of the linear size distribution. Unlike the networks from the 2D construction, networks from the 3D construction would not be nearly planar, and it would be of interest to investigate patterns in the clustering coefficient. In contrast, the same construction would not work in the 1D RTIM: Since the boundary of a connected region is constant, all connected node regions are expected to have equal average degree. A caveat is that for a 1D RTIM at criticality, there are logarithmic corrections to the area law<sup>72–74</sup>; however, it would be unwieldy to create power-law distributions from merely logarithmic corrections.

In conclusion, we have presented a way to create model complex quantum networks on a lattice of spins. As the first application, our work centers around the critical two-dimensional RTIM, but generalizations to other interacting spin systems with strong disorder that admit entangled ground state clusters are apparent. Our model serves as an accessible generative framework for further investigations on network complexity in the emerging quantum internet. Further, our results could motivate experimental work to create a spatially small but many-node complex

quantum communication network using a magnetic solid that admits magnetic domains in the form of spin clusters. We believe that in addition to ongoing and future experiments with a few nodes separated at large distances<sup>2,13–15</sup>, we also need small-scale experiments with many nodes to explore the implications of complex network topologies. This is an exciting time to explore the question of quantum network topology, influencing how the quantum internet will be shaped. As of now, it is unclear if the emerging quantum internet will acquire a complex network structure. Even if the quantum internet falls into a novel class of complex networks substantially different from those observed in classical systems, models like the one presented here may be valuable to understand how network properties arise.

#### Data availability

Data on the topology of the classical internet at the autonomous systems level are available from <https://snap.stanford.edu/data/as-733.html>. The rest of the data that support the findings of this study are available upon reasonable request.

#### Code availability

Codes developed in this work are available from the corresponding author upon reasonable request.

Received: 16 December 2022; Accepted: 14 September 2023;  
Published online: 26 September 2023

#### References

- Kimble, H. J. The quantum internet. *Nature* **453**, 1023–1030 (2008).
- Wehner, S., Elkouss, D. & Hanson, R. Quantum internet: a vision for the road ahead. *Science* **362**, eaam9288 (2018).
- Kozłowski, W. & Wehner, S. Towards large-scale quantum networks. In *Proc. Sixth Annu. ACM Int. Conf. Nanoscale Comput. Commun.*, NANOCOM '19, 1–7 (Association for Computing Machinery, New York, NY, USA, 2019).

4. Cacciapuoti, A. S. et al. Quantum internet: networking challenges in distributed quantum computing. *IEEE Netw.* **34**, 137–143 (2020).
5. van Leent, T. et al. Entangling single atoms over 33 km telecom fibre. *Nature* **607**, 69–73 (2022).
6. Luo, X.-Y. et al. Postselected entanglement between two atomic ensembles separated by 12.5 km. *Phys. Rev. Lett.* **129**, 050503 (2022).
7. Wei, S.-H. et al. Towards real-world quantum networks: a review. *Laser Photonics Rev.* **16**, 2100219 (2022).
8. Chen, J.-P. et al. Sending-or-not-sending with independent lasers: secure twin-field quantum key distribution over 509 km. *Phys. Rev. Lett.* **124**, 070501 (2020).
9. Fang, X.-T. et al. Implementation of quantum key distribution surpassing the linear rate-transmittance bound. *Nat. Photonics* **14**, 422–425 (2020).
10. Yin, J. et al. Satellite-based entanglement distribution over 1200 kilometers. *Science* **356**, 1140–1144 (2017).
11. Liao, S.-K. et al. Satellite-to-ground quantum key distribution. *Nature* **549**, 43–47 (2017).
12. Ren, J.-G. et al. Ground-to-satellite quantum teleportation. *Nature* **549**, 70–73 (2017).
13. Peev, M. et al. The SECOQC quantum key distribution network in Vienna. *New J. Phys.* **11**, 075001 (2009).
14. Sasaki, M. et al. Field test of quantum key distribution in the Tokyo QKD Network. *Opt. Express* **19**, 10387–10409 (2011).
15. Liao, S.-K. et al. Satellite-relayed intercontinental quantum network. *Phys. Rev. Lett.* **120**, 030501 (2018).
16. Biamonte, J., Faccin, M. & De Domenico, M. Complex networks from classical to quantum. *Commun. Phys.* **2**, 1–10 (2019).
17. Acín, A., Cirac, J. I. & Lewenstein, M. Entanglement percolation in quantum networks. *Nat. Phys.* **3**, 256–259 (2007).
18. Cirac, J. I., Zoller, P., Kimble, H. J. & Mabuchi, H. Quantum state transfer and entanglement distribution among distant nodes in a quantum network. *Phys. Rev. Lett.* **78**, 3221–3224 (1997).
19. Satoh, T., Le Gall, F. & Imai, H. Quantum network coding for quantum repeaters. *Phys. Rev. A* **86**, 032331 (2012).
20. Perseguers, S., Cirac, J. I., Acín, A., Lewenstein, M. & Wehr, J. Entanglement distribution in pure-state quantum networks. *Phys. Rev. A* **77**, 022308 (2008).
21. Schoute, E., Mancinska, L., Islam, T., Kerenidis, I. & Wehner, S. Shortcuts to quantum network routing. Preprint at *arXiv* <https://doi.org/10.48550/arXiv.1610.05238> (2016).
22. Meignant, C., Markham, D. & Grosshans, F. Distributing graph states over arbitrary quantum networks. *Phys. Rev. A* **100**, 052333 (2019).
23. Pirandola, S. End-to-end capacities of a quantum communication network. *Commun. Phys.* **2**, 1–10 (2019).
24. Shi, S. & Qian, C. Concurrent entanglement routing for quantum networks: model and designs. In *Proc. Annu. Conf. ACM Spec. Interest Group Data Commun. Appl. Technol. Archit. Protoc. Comput. Commun.*, SIGCOMM '20, 62–75 (Association for Computing Machinery, New York, NY, USA, 2020).
25. Barabási, A.-L. *Network Science* (Cambridge University Press, Cambridge, United Kingdom, 2016), 1st edition edn.
26. Albert, R., Jeong, H. & Barabási, A.-L. Error and attack tolerance of complex networks. *Nature* **406**, 378–382 (2000).
27. Coutinho, B. C., Munro, W. J., Nemoto, K. & Omar, Y. Robustness of noisy quantum networks. *Commun. Phys.* **5**, 1–9 (2022).
28. Sundar, B., Walschaers, M., Parigi, V. & Carr, L. D. Response of quantum spin networks to attacks. *J. Phys. Complex.* **2**, 035008 (2021).
29. Brito, S., Canabarro, A., Cavalcanti, D. & Chaves, R. Satellite-based photonic quantum networks are small-world. *PRX Quantum* **2**, 010304 (2021).
30. Rabbie, J., Chakraborty, K., Avis, G. & Wehner, S. Designing quantum networks using preexisting infrastructure. *npj Quantum Inf.* **8**, 1–12 (2022).
31. Brito, S., Canabarro, A., Chaves, R. & Cavalcanti, D. Statistical properties of the quantum internet. *Phys. Rev. Lett.* **124**, 210501 (2020).
32. Zhang, B. & Zhuang, Q. Quantum internet under random breakdowns and intentional attacks. *Quantum Sci. Technol.* **6**, 045007 (2021).
33. Zhuang, Q. & Zhang, B. Quantum communication capacity transition of complex quantum networks. *Phys. Rev. A* **104**, 022608 (2021).
34. Kovács, I. A. & Iglói, F. Renormalization group study of random quantum magnets. *J. Phys.* **23**, 404204 (2011).
35. Kovács, I. A. & Iglói, F. Renormalization group study of the two-dimensional random transverse-field Ising model. *Phys. Rev. B* **82**, 054437 (2010).
36. Motrunich, O., Mau, S.-C., Huse, D. A. & Fisher, D. S. Infinite-randomness quantum Ising critical fixed points. *Phys. Rev. B* **61**, 1160–1172 (2000).
37. Pich, C., Young, A. P., Rieger, H. & Kawashima, N. Critical behavior and Griffiths-McCoy singularities in the two-dimensional random quantum Ising ferromagnet. *Phys. Rev. Lett.* **81**, 5916–5919 (1998).
38. Lin, Y.-C., Kawashima, N., Iglói, F. & Rieger, H. Numerical renormalization group study of random transverse Ising models in one and two space dimensions. *Progr. Theor. Phys. Suppl.* **138**, 479–488 (2000).
39. Yu, R., Saleur, H. & Haas, S. Entanglement entropy in the two-dimensional random transverse field Ising model. *Phys. Rev. B* **77**, 140402 (2008).
40. Kovács, I. A. & Iglói, F. Critical behavior and entanglement of the random transverse-field Ising model between one and two dimensions. *Phys. Rev. B* **80**, 214416 (2009).
41. Lin, Y.-C., Iglói, F. & Rieger, H. Entanglement entropy at infinite-randomness fixed points in higher dimensions. *Phys. Rev. Lett.* **99**, 147202 (2007).
42. Kovács, I. A. & Juhász, R. Emergence of disconnected clusters in heterogeneous complex systems. *Sci. Rep.* **10**, 21874 (2020).
43. Kovács, I. A. & Iglói, F. Universal logarithmic terms in the entanglement entropy of 2d, 3d and 4d random transverse-field Ising models. *EPL* **97**, 67009 (2012).
44. Bianconi, G. Superconductor-insulator transition in a network of 2d percolation clusters. *EPL* **101**, 26003 (2013).
45. Iglói, F. & Monthus, C. Strong disorder RG approach of random systems. *Phys. Rep.* **412**, 277–431 (2005).
46. Iglói, F. & Monthus, C. Strong disorder RG approach—a short review of recent developments. *Eur. Phys. J. B* **91**, 290 (2018).
47. Sachdev, S. Quantum criticality: competing ground states in low dimensions. *Science* **288**, 475–480 (2000).
48. Sachdev, S. *Quantum Phase Transitions* (Cambridge University Press, Cambridge, 2011), second edn.
49. Ma, S.-K., Dasgupta, C. & Hu, C.-K. Random antiferromagnetic chain. *Phys. Rev. Lett.* **43**, 1434–1437 (1979).
50. Dasgupta, C. & Ma, S.-K. Low-temperature properties of the random Heisenberg antiferromagnetic chain. *Phys. Rev. B* **22**, 1305–1319 (1980).
51. Fisher, D. S. Phase transitions and singularities in random quantum systems. *Physica A* **263**, 222–233 (1999).
52. Karevski, D., Lin, Y.-C., Rieger, H., Kawashima, N. & Iglói, F. Random quantum magnets with broad disorder distribution. *Eur. Phys. J. B* **20**, 267–276 (2001).
53. Kovács, I. A. & Iglói, F. Infinite-disorder scaling of random quantum magnets in three and higher dimensions. *Phys. Rev. B* **83**, 174207 (2011).
54. Refael, G. & Moore, J. E. Entanglement entropy of random quantum critical points in one dimension. *Phys. Rev. Lett.* **93**, 260602 (2004).
55. Eisert, J., Cramer, M. & Plenio, M. B. Colloquium: area laws for the entanglement entropy. *Rev. Mod. Phys.* **82**, 277–306 (2010).
56. Wang, W., Wang, H., Dai, G. & Wang, H. Visualization of large hierarchical data by circle packing. In *Proc. SIGCHI Conf. Hum. Factors Comput. Syst.*, CHI '06, 517–520 (Association for Computing Machinery, New York, NY, USA, 2006).
57. Szalay, Sz. Multipartite entanglement measures. *Phys. Rev. A* **92**, 042329 (2015).
58. Vidal, G. & Werner, R. F. Computable measure of entanglement. *Phys. Rev. A* **65**, 032314 (2002).
59. Plenio, M. B. Logarithmic negativity: a full entanglement monotone that is not convex. *Phys. Rev. Lett.* **95**, 090503 (2005).
60. Ruggiero, P., Alba, V. & Calabrese, P. Entanglement negativity in random spin chains. *Phys. Rev. B* **94**, 035152 (2016).
61. Zou, J. S., Ansell, H. S. & Kovács, I. A. Multipartite entanglement in the random Ising chain. *Phys. Rev. B* **106**, 054201 (2022).
62. Meyer, D. Route Views—University of Oregon Route Views Project. <http://www.routeviews.org/routeviews/>.
63. Ravasz, E. & Barabási, A.-L. Hierarchical organization in complex networks. *Phys. Rev. E* **67**, 026112 (2003).
64. Senthil, T. & Sachdev, S. Higher dimensional realizations of activated dynamic scaling at random quantum transitions. *Phys. Rev. Lett.* **77**, 5292–5295 (1996).
65. Harris, A. B. Effect of random defects on the critical behaviour of Ising models. *J. Phys. C* **7**, 1671–1692 (1974).
66. Stinchcombe, R. B. Diluted quantum transverse Ising model. *J. Phys. C* **14**, L263–L267 (1981).
67. dos Santos, R. R. The pure and diluted quantum transverse Ising model. *J. Phys. C* **15**, 3141–3161 (1982).
68. Senthil, T. & Aharony, S. N. Critical properties of random quantum Potts and clock models. *Phys. Rev. Lett.* **76**, 3001–3004 (1996).
69. Carlon, E., Lajkó, P. & Iglói, F. Disorder induced cross-over effects at quantum critical points. *Phys. Rev. Lett.* **87**, 277201 (2001).
70. Stauffer, D. & Aharony, A. *Introduction To Percolation Theory: Second Edition* (Taylor & Francis, London, 2017), second edn.
71. Kivelä, M. et al. Multilayer networks. *J. Complex Netw.* **2**, 203–271 (2014).
72. Holzhley, C., Larsen, F. & Wilczek, F. Geometric and renormalized entropy in conformal field theory. *Nucl. Phys. B* **424**, 443–467 (1994).
73. Vidal, G., Latorre, J. I., Rico, E. & Kitaev, A. Entanglement in quantum critical phenomena. *Phys. Rev. Lett.* **90**, 227902 (2003).
74. Calabrese, P. & Cardy, J. Entanglement entropy and quantum field theory. *J. Stat. Mech.* P06002 (2004).

## Acknowledgements

This work was supported by the National Science Foundation under Grant No. PHY-2310706 of the QIS program in the Division of Physics, the JTF project *The Nature of Quantum Networks* (ID 60478), and the Baker Faculty Grant of the Weinberg College of Arts and Sciences, Northwestern University, 2020. R.T.C. Chepuri was supported by the Northwestern University SURG-Advanced in 2021. We are thankful for Ginestra Bianconi for useful discussions. We also thank Bingjie Hao, Anastasiya Salova, and Helen S. Ansell for insightful feedback on the manuscript.

## Author contributions

I.A.K. developed the initial concept and supervised the research. R.T.C.C. performed the network simulations and numerical analyses. All authors contributed to the design and writing of the manuscript.

## Competing interests

The authors declare no competing interests.

## Additional information

**Supplementary information** The online version contains supplementary material available at <https://doi.org/10.1038/s42005-023-01394-8>.

**Correspondence** and requests for materials should be addressed to István A. Kovács.

**Peer review information** *Communications Physics* thanks Bhuvanesh Sundar, Bingzhi Zhang and the other, anonymous, reviewer(s) for their contribution to the peer review of this work. A peer review file is available.

**Reprints and permission information** is available at <http://www.nature.com/reprints>

**Publisher's note** Springer Nature remains neutral with regard to jurisdictional claims in published maps and institutional affiliations.



**Open Access** This article is licensed under a Creative Commons Attribution 4.0 International License, which permits use, sharing, adaptation, distribution and reproduction in any medium or format, as long as you give appropriate credit to the original author(s) and the source, provide a link to the Creative Commons license, and indicate if changes were made. The images or other third party material in this article are included in the article's Creative Commons license, unless indicated otherwise in a credit line to the material. If material is not included in the article's Creative Commons license and your intended use is not permitted by statutory regulation or exceeds the permitted use, you will need to obtain permission directly from the copyright holder. To view a copy of this license, visit <http://creativecommons.org/licenses/by/4.0/>.

© The Author(s) 2023